

Review

Biophysical Aspects of Neurodegenerative and Neurodevelopmental Disorders Involving Endo-/Lysosomal CLC Cl⁻/H⁺ Antiporters

Maria Antonietta Coppola^{1,2}, Abraham Tettey-Matey¹, Paola Imbrici², Paola Gavazzo¹, Antonella Liantonio² and Michael Pusch^{1,3,*}

¹ Istituto di Biofisica, Consiglio Nazionale delle Ricerche, 16149 Genova, Italy; maria.coppola@uniba.it (M.A.C.); masirlow@gmail.com (A.T.-M.); paola.gavazzo@ibf.cnr.it (P.G.)

² Department of Pharmacy–Drug Sciences, University of Bari “Aldo Moro”, 70125 Bari, Italy; paola.imbrici@uniba.it (P.I.); antonella.liantonio@uniba.it (A.L.)

³ RAISE Ecosystem, 16149 Genova, Italy

* Correspondence: michael.pusch@ibf.cnr.it

Abstract: Endosomes and lysosomes are intracellular vesicular organelles with important roles in cell functions such as protein homeostasis, clearance of extracellular material, and autophagy. Endolysosomes are characterized by an acidic luminal pH that is critical for proper function. Five members of the gene family of voltage-gated Chloride Channels (CLC proteins) are localized to endolysosomal membranes, carrying out anion/proton exchange activity and thereby regulating pH and chloride concentration. Mutations in these vesicular CLCs cause global developmental delay, intellectual disability, various psychiatric conditions, lysosomal storage diseases, and neurodegeneration, resulting in severe pathologies or even death. Currently, there is no cure for any of these diseases. Here, we review the various diseases in which these proteins are involved and discuss the peculiar biophysical properties of the WT transporter and how these properties are altered in specific neurodegenerative and neurodevelopmental disorders.

Keywords: CLC proteins; endosome; lysosome; chloride transport; developmental



Citation: Coppola, M.A.; Tettey-Matey, A.; Imbrici, P.; Gavazzo, P.; Liantonio, A.; Pusch, M. Biophysical Aspects of Neurodegenerative and Neurodevelopmental Disorders Involving Endo-/Lysosomal CLC Cl⁻/H⁺ Antiporters. *Life* **2023**, *13*, 1317. <https://doi.org/10.3390/life13061317>

Academic Editor: Carlo Musio

Received: 22 May 2023

Revised: 30 May 2023

Accepted: 31 May 2023

Published: 2 June 2023



Copyright: © 2023 by the authors. Licensee MDPI, Basel, Switzerland. This article is an open access article distributed under the terms and conditions of the Creative Commons Attribution (CC BY) license (<https://creativecommons.org/licenses/by/4.0/>).

1. Introduction—The CLC Family

Physiologically, the most abundant anion is chloride. It is an important substrate of many transport proteins, being carried across the membrane as a single anion or coupled with other ions, and is important, for example, for the regulation of the membrane potential, intracellular vesicles acidification and cell volume regulation [1].

In humans, the CLC family is formed by nine members, which had initially been supposed to be all chloride channels, because of their sequence homology with the founding member, the *Torpedo* electroplax channel CIC-0 [2]. The discovery that the bacterial *Escherichia coli* eCIC-1 homologue is not a passive chloride channel but a stoichiometrically coupled secondary active 2 Cl⁻/1 H⁺ antiporter has dramatically changed the point of view of the entire CLC group [3]. Based on sequence homology, three branches of human CLCs have been distinguished. The first one includes the plasma membrane-localized chloride channels CIC-1, CIC-2 and the two isoforms CIC-Ka and CIC-Kb. The second branch is formed by CIC-3, CIC-4 and CIC-5, while the third branch contains CIC-6 and CIC-7. CIC-3 to -7 are all Cl⁻/H⁺ exchangers and are localized to the intracellular membranes of endosomes and/or lysosomes [1].

All CLC family members share the same dimeric architecture that is unique to this protein family. Except for CIC-6 and CIC-7 [4], the other CLC proteins can form homo- or hetero-dimers with members of the same branch [1]. Biochemical studies and single-channel analysis on the first cloned *Torpedo* CIC-0, mutants [2,5,6] and biochemical and low-resolution structural analysis of eCIC-1 [7,8] suggested a homodimeric “double-barreled”

architecture, with physically separated anion transport pathways in each protomer. This architecture has been fully confirmed by the determination of ecClC-1 and *Salmonella typhimurium* stClC crystal structures [9,10]. The structures revealed the presence of distinct anion binding sites, formed by residues that are also highly conserved in human CLCs. The sites are denominated Sext, Scen and Sint, with Sext being occupied by the presumably negatively charged side chain of the “gating glutamate” E148 [9,10]. Each monomer presents 18 α -helices (from A to R) of which 17 are partially embedded in the membrane. The two subunits interact in a tight manner and the architecture follows an inverted and parallel orientation [1]. Two C-terminal tandem cystathionine- β -synthase (CBS) domains are present in most eukaryotic CLC proteins [11,12], but are absent in ecClC-1. The two CBS domains may have a role in the so-called common gating process (that will be discussed in more detail below) and confer unique features to the CLC members [1]. Dutzler and colleagues determined the crystal structures of isolated CBS domains of *Torpedo* ClC-0 [13], human ClC-5 [14] and human ClC-Ka [15]. CBS domains are present in many different protein families, where they are often implicated in the sensing of adenine nucleotides [11,16]. Structurally, so far, ATP has been found to be bound in the isolated domains of ClC-5 and in the full-length structure of ClC-7 [17], but not in isolated domains of ClC-0 and ClC-Ka and not in full-length structures of bovine ClC-K or human ClC-1 [18–20].

Single-channel recordings of the *Torpedo* ClC-0 channel displayed two kinds of gating mechanisms that regulate the open probability (P_o) of the channel: a “fast” or “protopore” gate that acts independently on single pores determines the closing or opening state of each pore of the double-barreled structure [1]. The fast gate is mainly determined by the gating glutamate (E166 in ClC-0), in that its neutralization renders CLC-0 channels voltage independent. Protonation of the gating glutamate and its competition with permeant ions underlie the anion and pH dependent protopore gating of most CLC channels [10,21–23]. Conversely, a second mechanism, termed a *slow* or *common* gate, operates on both pores simultaneously and is still not well understood [1].

Some CLC proteins require association with a small ancillary subunit for proper function or membrane expression. In particular, the kidney ClC-Ka and ClC-Kb channels require association with the barttin subunit [24]. In glia cells, ClC-2 associates with GlialCAM, a protein with the typical architecture of a cell adhesion molecule, which is mutated in megalencephalic leukoencephalopathy with subcortical cysts (MLC) [25]. It leads to clustering of ClC-2 at glial cell–cell contacts and alters biophysical functions of the ClC-2 channel [25,26]. The complex of ClC-7 with its subunit Ostm1 is mandatory for mutual stabilization [4,27].

The plasma membrane localized chloride channels belonging to the first branch of the CLC family are expressed in a tissue-dependent manner that is different for each member according to their physiological role. All channel CLCs are involved in various human genetic diseases, as reviewed in detail elsewhere [1,28,29].

ClC-3 through ClC-7, which are the focus of this review, function as Cl^-/H^+ exchangers and are localized to intracellular endosomes and/or lysosomes (Figure 1, Table 1). Initially, when the transporter function of the intracellular CLCs was not yet known, it was proposed that they act as charge-shunting chloride channels to assist the luminal acidification of endosomes and lysosomes intracellular organelles [30–34]. Indeed, the maintenance of an acidic pH of the lumen of endo-/lysosomes is required for their proper physiological function. The proton pumping V-ATPase is electrogenic and thus generates an electrical potential difference that would impede acidification if not neutralized by anionic cotransport and/or cationic counter-transport. Somewhat surprisingly and counter-intuitively, model calculations show that a 2 Cl^-/H^+ exchange activity, contributing to a more inside-negative voltage, allows a more acidic steady-state luminal pH compared to a shunting Cl^- channel [35,36].

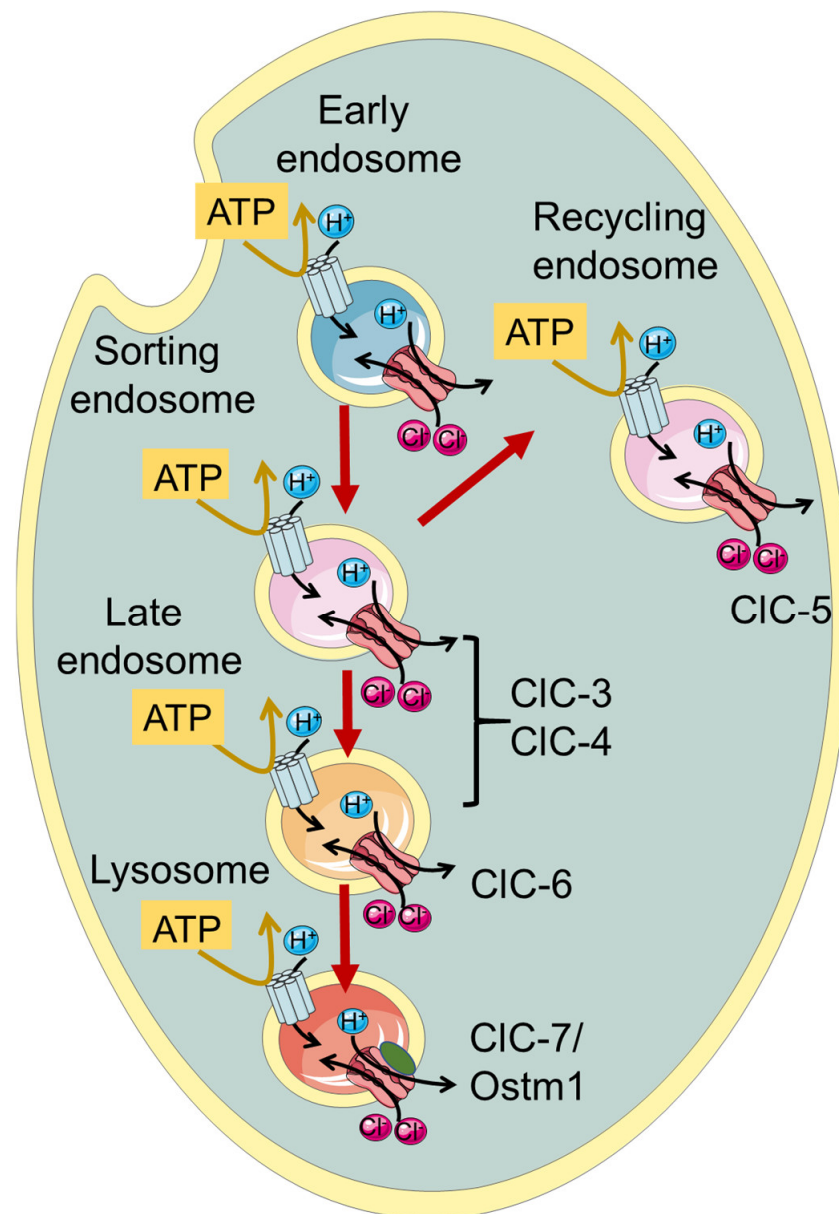


Figure 1. Schematic illustration of localization of vesicular CLCs in the endo-/lysosomal pathway.

Among the endo-/lysosomal CLCs, CIC-5 is rather specifically expressed in the kidney with a predominant presence in epithelial cells of the proximal tubule, where it is involved in endocytic uptake [30,31,33]. Indeed, mutations causing impaired CIC-5 transport activity are associated with Dent's disease, a kidney disorder characterized by the primary symptom of low molecular weight proteinuria, and a series of secondary symptoms including kidney stones and renal failure, caused by defective endocytosis in the proximal tubule [33,37]. CIC-7, together with its subunit Ostm1 [27], is rather ubiquitously expressed in the body and is localized to lysosomes and in the ruffled border of osteoclasts functioning as a $2\text{Cl}^-/\text{H}^+$ antiporter [1]. Accordingly, impaired bone resorption in osteoclast, caused by a functionally defective CIC-7/Ostm1 complex, causes osteopetrosis, a disease characterized by stiff and fragile bones [38].

Table 1. List of the CLC genes, subcellular localization and CLC related neurological diseases.

Protein	Gene	Cellular Localization	Neurological Disorder	Symptoms	References
CIC-3	<i>CLCN3</i>	Sorting and late endosomes	Global developmental delay	Intellectual disability, agenesis of the corpus callosum, epilepsy, visual impairment, hypotonia, anxiety, dysmorphic facial features	[39]
CIC-4	<i>CLCN4</i>	Sorting and late endosomes	<i>CLCN4</i> -related X linked intellectual disability syndrome	Intellectual disability, epilepsy, autism, growth and feeding difficulties, epilepsy, movement disorders, gastrointestinal conditions, dysmorphic facial features	[40–42]
CIC-6	<i>CLCN6</i>	Late endosomes	Early Onset Neurodegeneration	Severe neurodegeneration, severe generalized hypotonia and respiratory insufficiency, brain atrophy	[43]
			Kufs' disease	Adult-onset neuronal ceroid Lipofuscinosis, movement and cognitive function impairment	[44,45]
			West syndrome	Severe developmental delay, autism, movement disorder, microcephaly, facial dysmorphism, visual impairment	[46]
CIC-7/ Ostm1	<i>CLCN7</i> / <i>OSTM1</i>	Lysosomes	Autosomal Recessive Osteopetrosis	Osteopetrosis, lysosomal storage disease, neurodegeneration, visual impairment	[38,47,48]
			Gain of function <i>CLCN7</i> related disease	Delayed myelination and development, organomegaly, and hypopigmentation	[49]

A large phenotypic spectrum of neuronal diseases is associated with mutations in the genes encoding CIC-3/-4/-6 and CIC-7, as will be described in detail in the following paragraphs (see Table 1).

For all vesicular CLCs, an unsolved question pertains to the direction of exchanger transport. Despite being physiologically localized to endo-/lysosomes, CIC-3 to -6 can reach the plasma membrane when heterologously expressed in HEK293 cells, allowing the investigation of their biophysical properties using the patch clamp technique [45,50–53]. For CIC-7, the elimination of N-terminal lysosomal targeting motifs leads to plasma membrane expression [4,54]. CIC-3 to -5 all exhibit extreme outward rectification of currents with very little or nonresolvable activation kinetics [50–53,55]. This current direction corresponds to the transport of luminal Cl[−] out of lysosomes with a parallel influx of cytosolic H⁺. However, it remains unclear whether the direction of transport is physiologically relevant and whether CLC exchangers work synergistically with V-ATPase, contributing to luminal acidification.

Additionally, CIC-6 and CIC-7 exhibit strongly outwardly rectifying currents, which are, however, characterized by slow activation kinetics and measurable inward “tail” currents [4,45].

2. CIC-3 and CIC-4

The second branch of the CLC family comprises CIC-3, -4 and 5. These three endosomal transporters share high sequence similarity and have similar functional properties [1,29]. Among the human CLCs, they are the most similar to the *Escherichia coli* ecCIC-1 homologue. The renal-specific CIC-5 is found mostly in recycling endosomes and its physiological role will not be discussed in detail [1]. CIC-3 and CIC-4 are localized to sorting endosomes, and

CIC-3 is probably localized in late endosomes as well [1,29]. CIC-3 has also been proposed to play a role in synaptic vesicles. This is, however, still controversial and will not be discussed in detail here (see [29] for a discussion).

Functionally, these transporters are characterized by an extremely outwardly rectifying current–voltage relationship with almost instantaneous activation at positive voltages [50–52,55–58] (Figure 2A). The extreme outward rectification precluded the determination of transport stoichiometry by reversal potentials measurements [59]. Using a fluorescent assay, a $2 \text{ Cl}^- / 1 \text{ H}^+$ stoichiometry was determined for CIC-5, which is probably similar for CIC-3 and CIC-4 [55]. The outward rectification at least partially reflects a gating process, as evidenced by a single point mutation (D76H) that conferred detectable inward tail currents to CIC-5 [60]. The mutant also allowed us to measure reversal potentials for CIC-5 for the first time, confirming the $2:1 \text{ Cl}^- / \text{H}^+$ transport stoichiometry [60].

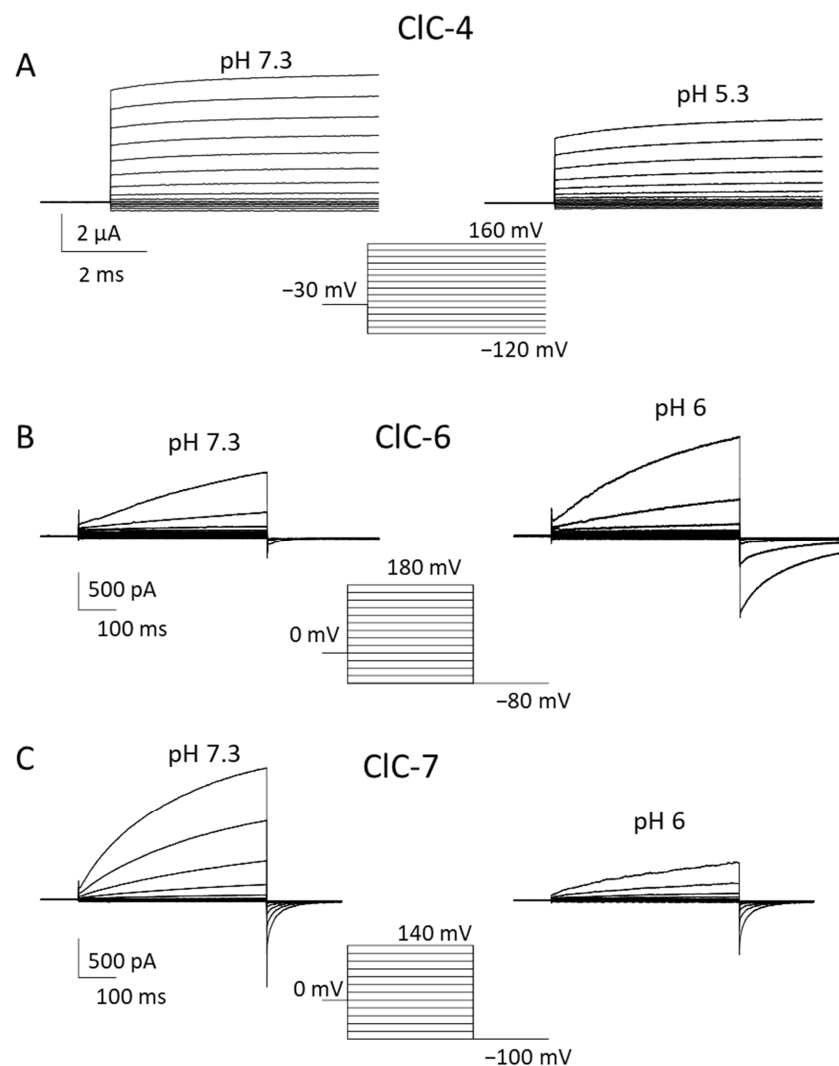


Figure 2. Biophysical properties of CIC-4, CIC-6 and CIC-7. Typical voltage-clamp current traces of CIC-4 ((A), expressed in *Xenopus* oocytes), CIC-6 ((B), expressed in HEK cells), and CIC-7^{PM} ((C), expressed in HEK cells), elicited by the indicated voltage-clamp protocols, measured using the two-electrode voltage clamp method (A) or the whole-cell recording mode of the patch clamp technique (B,C) at neutral (left panels) and acidic (right panels) pH. Extracellular solutions were 100 mM NaCl, 10 mM Hepes or MES, 5 mM MgSO₄ (A) or 150 mM NaCl, 10 mM Hepes or MES, 4 mM MgSO₄ (B,C). In B and C the pipette solution contained 130 mM NaCl, 10 mM Hepes, 2 mM EGTA, 2 mM MgSO₄. CIC-3 is similar to CIC-4.

Most evidence on the physiological roles of CIC-3 and CIC-4 was obtained from mouse models and their involvement in human genetic diseases. CIC-3 KO mice display severe postnatal neurodegeneration with almost total loss of the hippocampus after 3 months [34,61,62]. Yet, CIC-3 KO mice have a normal life span. Neurodegeneration is unlikely to be caused by impaired synaptic function [1,29]. Another set of mouse models showed that CIC-4 protein stability relies on the presence of CIC-3 via heterodimerization [63,64]. While CIC-4 KO mice have no overt phenotype, the double KO of CIC-3 and CIC-4 has a more severe phenotype than CLC-3 KO mice [64]. Notably, differently from humans, *Clcn4* is not X-linked in laboratory mice. For this reason, a rat model might be more useful for the investigation of mechanisms underlying *CLCN4*-related disease, because in rats, as in humans, *Clcn4* is X-linked.

While CIC-4 KO mice have no overt phenotype, in 2013 and 2016, patients (mostly pediatric) with a range of neurodevelopmental and psychiatric complications have been described with X-linked *CLCN4* variants [40,42,65] (see Table 1). In heterologous expression, these and some novel variants [66] showed variable loss of function effects. It is important to note that complete loss of CIC-4 protein leads to non-syndromic intellectual disability in males and no disease in heterozygous females. In contrast, de novo and inherited missense variants can lead to severe syndromic neurological disease in males as well as in females, suggesting a dominant effect. In a recent study, a large number of *CLCN4* families was investigated, describing a large spectrum of clinical phenotypes and studying > 50 missense variants in heterologous expression [41]. Novel biophysical mechanisms were discovered for new and already described variants. These included a toxic gain of function characterized by the presence of negative currents at acidic extracellular (luminal) pH, and a shift in the voltage dependence of gating to more positive voltages [41]. Both effects can be expected to exert dominant negative effects in CIC-3/CIC-4 heterodimers.

Almost simultaneously came the discovery of the first variants in *CLCN3* that cause global developmental delay, intellectual disability and neurodevelopmental disorders [39] (Table 1). Detailed functional analysis revealed a toxic gain of function for two missense variants, similar to the above-described effects in some *CLCN4* variants [39].

3. CIC-6

The third branch of the CLC family comprises CIC-6 and CIC-7, which both function as Cl^-/H^+ exchangers [1,45]. Even though the expression of CIC-6 mRNA appears to be ubiquitous in many tissues [67], biochemical analysis detected native CIC-6 protein predominantly in neurons, where it localizes to late endosomes and partially lysosomes [44]. For a long time, the biophysical profile of CIC-6 remained completely unknown. In the first attempts at heterologous expression, no currents attributable to CIC-6 could be detected [67], possibly caused by the intracellular localization of most of the overexpressed protein [68].

A subtype of lysosomal storage disease, referred to as neuronal ceroid lipofuscinosis (NCL), was observed in CIC-6 *knockout* mice presenting a mild phenotype with features of reduced pain sensitivity, probably due to strong accumulation of materials in axon initial segments, mild cognitive abnormalities and no impact on their span life [44]. This evidence suggested that *CLCN6* variants could be involved in human NCL [44]. Indeed, in a sample of 75 adult-onset variants, including late-onset forms of NLC and Kufs' disease, two individuals were found to be heterozygous for *CLCN6* missense variants (V580M and T628R) [44]. However, no functional analysis had been performed at the time of that study because the transporter had not been successfully functionally characterized.

Preliminary electrophysiological characterization was obtained when the N-terminus of CIC-6 tagged with GFP (GFP-CIC-6) was reported to enhance its cell surface localization [69]. However, the reported currents were small and barely above background levels.

In 2020, the same de novo variant in *CLCN6* leading to the amino acid change Y553C was reported in three pediatric patients with no parental correlation [43]. The patients exhibited a severe syndrome characterized by early-onset neurodegeneration. The mutated tyrosine, located in the extracellular P-Q loop, is highly conserved among CLC antiporters.

Electrophysiological measurements of CIC-6^{Y553C} revealed large currents activated at positive voltages (≥ 60 mV), representing a clear gain of function effect [43]. HEK cells overexpressing the mutant showed a dramatic vacuolization [43]. The luminal pH of these organelles did not reach low values, suggesting that the mutant impairs endolysosomal ionic homeostasis in patients.

In 2022, Zifarelli et al. were able to obtain robust recordings of WT CIC-6 currents by applying very large positive voltages beyond 140 mV [45,70]. Interestingly, the magnitude and properties of currents were independent of the N-terminal GFP tag. Similar to CIC-7, CIC-6-mediated currents showed slow activation at positive voltages; however, they required voltages of at least 140 mV to measure appreciable amplitudes [45] (Figure 2B). The necessity of the large voltages explained why these currents had escaped detection so far. Currents represent the coupled Cl^-/H^+ antiport, as assayed by reversal potential measurements [45]. Similar to CIC-7 [71], CIC-6 also exhibits so called “transient” or “capacitive” currents, whose possible physiological role is, however, obscure [45]. Interestingly, neutralizing the so-called proton glutamate did not completely abolish transport currents [45]. In contrast to most other CLC proteins, CIC-6-mediated currents were enhanced at acidic pH (6.3) compared to neutral pH [45] (Figure 2B), a finding that is of likely physiological relevance. In light of these novel findings on the functional properties of CIC-6, Zifarelli et al. performed a reexamination of the disease-causing variant CIC-6^{Y553C}, concluding that the mutation causes a gain of function by “shifting” the voltage dependence of CIC-6 gating to less positive voltages [45]. Possibly, Y553, being localized at the subunit interface of the homodimer, is involved in the common gating mechanism that acts on both ion-transporting units of the dimer.

The discovery of suitable recording protocols allowed Zifarelli et al. to study the functional impact of the two above-mentioned variants found in Kufs’ disease patients. While T628R was indistinguishable from WT CIC-6, precluding firm conclusions regarding its causative nature for the disease, variant V580M showed a clearly reduced function, suggesting a causal relationship [45]. Since the variant was found in heterozygosity, it might exert a dominant negative effect in WT/mutant heterodimers.

Patients with the completely unrelated West syndrome, characterized by epilepsy, among other symptoms, have been reported to carry the CIC-6 E200A variant [46]. E200 is the critical gating glutamate of the exchanger and it is known that its neutralization in all studied vCLCs, including CIC-6, eliminates H^+ transport and transforms it into an uncoupled ohmic chloride channel [69]. In a heterologous expression system, CIC-6^{E200A} caused an impairment of the autophagosome-mediated degradation system, likely because the fusion with lysosomes was compromised [46].

The three classes of disease related *CLCN6* mutations, i.e., gain of function (Y553C), reduction of function (V580M), and uncoupling (E200A), have different effects on the functional properties of the CIC-6 antiporter, leading to clinical phenotypes with different degrees of severity. In particular, CIC-6^{Y553C} causing a gain of function is associated with drastic neurodegeneration, whereas CIC-6^{E200A} could be defined as a loss of function in the respect of the uncoupling transport generated and related to a mild phenotype.

The recent remarkable progress that has been made regarding the functional analysis of CIC-6 activity will allow us to decode further mechanisms underlying disease caused by defective CIC-6 proteins.

4. CIC-7

Belonging to the third mammalian CLC branch, CIC-7 shares 45% of sequence homology with CIC-6. It was cloned in parallel with CIC-6 in 1995 [67], but could not be functionally analyzed for a long time. Intriguingly, CIC-7 is the only subcellular CLC member to be present almost exclusively in lysosomes [44]. Moreover, it has also been found in the ruffled border of osteoclasts, where it participates in bone resorption [38]. Unlike the other CLC transporters, CIC-7 requires association with a type I transmembrane protein, called Ostm1, for proper function and stability [4,27].

Similarly to CIC-6, no information about electrophysiological CIC-7 characterization has been available for a long time, due to its intracellular localization upon heterologous expression [1]. Ion flux studies with isolated mouse lysosomes showed that CIC-7 is the dominant anion permeation pathway of lysosomal membranes and that it performs $2 \text{ Cl}^- / 1 \text{ H}^+$ antiport activity [72]. A breakthrough was achieved by Stauber and Jentsch, who discovered the sorting motifs that mediate lysosomal targeting [54]. In particular, they found that when four leucine residues localized in the N-terminal portion are changed to alanine, the transporter is at least partially targeted to the plasma membrane [54]. Notably, *Ostm1* follows CIC-7 in its expression location. CIC-7^{PM}, the CIC-7 variant in which the two dileucine motifs are mutated to alanine, elicited robust transmembrane, outwardly rectifying voltage-activated currents [4] (Figure 2C). Even though some electrophysiological properties of CIC-7 are similar to that of other vesicular CLCs, including the inhibitory effect of acidic pH, CIC-7 differs substantially from CIC-3 to -5. Most importantly, CIC-7^{PM} exhibits very slow activation kinetics in the seconds time range [4] (Figure 2C). This slow “gating” phenomenon is strictly linked to conformational changes in the proteins, where the interactions between transmembrane as well as cytoplasmic domains play a key role [73]. In addition to the transport currents, Pusch and Zifarelli discovered that the transporter also exhibits rather large “transient” or “capacitive” currents that reflect charge rearrangements within the protein. These are most likely mediated by movements of the gating glutamate and chloride binding/unbinding events [71]. Similar currents have been observed in CIC-5 and CIC-3 [52,74,75]. The transient currents probably have no physiological role, but represent a biophysical feature that can be useful in deciphering molecular mechanisms of gating and transport. Interestingly, while in CIC-5, neutralization of the so-called proton glutamate completely abolished transport currents, leaving only transient currents [74,75], in CIC-7, residual transport currents were observed in the corresponding E312A mutant [71].

The physiological role of CIC-7 remained unclear for a long time. The first insights were obtained with a mouse KO model that was characterized by severe osteopetrosis [38]. The involvement of CIC-7 in bone resorption was confirmed by the presence of *CLCN7* mutations in a human patient with malignant osteopetrosis [38]. Further evidence came from the identification of a spontaneous *Ostm1* mutation to be associated with the onset of a severe osteopetrosis in *gray lethal* mice presenting a fur color defect [76]. In *Clcn7*^{-/-} mice, even though the number of osteoclasts was normal, their ability to reabsorb calcified bone was impaired [38]. Interestingly, however, no impact on lysosomal acidification was observed, suggesting that the osteoclasts’ ability to acidify intracellular vesicles was preserved in *Clcn7*^{-/-} mice [38]. The life span of the KO mice was limited to 6–7 weeks.

Importantly, in addition to osteopetrosis, CIC-7^{-/-} mice also presented severe lysosomal storage associated with central nervous system and retinal degeneration [47]. Using a lacZ fusion protein, the expression profile of CIC-7 was determined in the nervous tissue of WT and KO mice revealing the hippocampus CA3 region, the cortex and the cerebellum as the main regions experiencing neuronal loss in KO mice [47]. Electron microscopy analysis revealed the presence of autofluorescent lipopigment in the regions affected by neurodegeneration and deficient of CLC-7 [47]. This factor, together with the detection of microglial activation and astrogliosis, represents three important hallmarks of neuronal ceroid lipofuscinosis (NCL) [47]. Importantly, no significant difference in pH values in lysosomes of cultured neurons and fibroblasts was found in *Clcn7*^{-/-} mice, but rather a reduction in lysosomal Cl concentration was observed [47]. Several pieces of evidence suggest that osteopetrosis and neurodegeneration are independent outcomes. First, an osteopetrotic mouse model with a mutation in the $\alpha 3$ subunit of V-type H⁺-ATPase (*oc/oc* mice) does not show retinal or neurodegeneration [47]. Moreover, the osteoporotic phenotype in *Clcn7*^{-/-} mice could be rescued by transgenically expressing CIC-7 in osteoclasts and macrophages under the control of tartrate-resistant acid phosphatase (TRAP) promoter [47]. This treatment achieved a lifespan increase, but it was not enough to ensure their survival due to the enduring neurological problems [47]. Surprisingly, the same approach failed when TRAP promoter-mediated *Ostm1* expression was applied to rescue osteopetrosis in *gray lethal*

(gl) mice which also displayed neuronal loss [77]. The severity of the phenotype and the short life span of the mice were serious problems, preventing a better understanding of the mechanisms underlying the progression of neurodegeneration in lysosomal pathologies [1]. The first information was collected when Wartosch et al. designed a floxed *Clcn7* mouse model allowing tissue-specific CLC-7 depletion [78]. No difference in lifespan between neuron-specific *Clcn7* KO and WT mice was observed. Moreover, neuron-specific *Clcn7* KO mice had no osteopetrotic phenotype; thus, the quality of life of these mice was improved compared to *Clcn7*^{-/-} [78]. Importantly, it was observed that neuronal loss occurs in regions, where CLC-7 had been disrupted and neurodegeneration started in the CA3 region of the hippocampus as in constitutive *Clcn7*^{-/-}. Accordingly, in previous studies, astrogliosis and microglia activation were observed in the regions lacking CLC-7. Impaired lysosomal protein degradation was suggested after the detection of increased levels of LC3-II, a marker of autophagy [78].

A somewhat surprising finding was that several, mostly dominantly inherited, *CLCN7* variants causing osteopetrosis (but not neurodegeneration) produce a significant acceleration of gating kinetics [4,79,80]. It is unclear how this biophysical defect is related to CLC-7 malfunction.

More recently, a completely different disease characterized by delayed myelination and development, organomegaly and hypopigmentation was found in two children who both carried the de novo Y715C variant [49]. Surprisingly, none of the patients showed osteopetrosis (see Table 1). The variant, located in the C-terminus, was associated with larger currents when directed to the plasma membrane, representing a clear gain of function effect. Interestingly, the lysosomes of patient fibroblasts were enlarged and had a lower pH (0.2 pH units) than control lysosomes [49]. Even more excitingly, in the CLC-7 structure, Y715 is relatively close to the bound PI(3)P molecule (see below) and Leray et al. recently reported that intracellular phosphatidylinositol-3,5-bisphosphate (PI(3,5)P₂) appears to tonically inhibit CLC-7 function, and that the Y715C variant was insensitive to PI(3,5)P₂ [81]. The regulation of CLC-transporters by these signaling molecules is clearly an exciting aspect that needs to be understood in more detail.

The structure of the CLC-7/Ostm1 complex has been determined by two independent groups [17,82]. The structures revealed that the heavily N-glycosylated luminal region of Ostm1 forms a sort of cap on the luminal portion of CLC-7, preventing its degradation by lysosomal proteases [17,82]. Importantly, the mutual protein stabilization between CLC-7 and Ostm1 is suggested by the observation that the gray lethal mouse line, which lacks Ostm1, showed very weak CLC-7 staining; similarly, in *Clcn7*^{-/-} mice, there was only weak Ostm1 staining [27,76]. Both cryo-EM structures revealed strong intramolecular interactions between the cytosolic N-terminal portion and the CBS domains [17,82]. This important feature is also conserved in CLC-6 (Hite, personal communication), but the role of these interactions in other CLCs remains unclear because no information about the cytosolic structure of other CLC members is available. Similarly to CLC-5, the CLC-7 CBS domains bind ATP and additionally, a Mg²⁺ ion was found to be bound [17,82]. However, ATP had no effect on transport activity and its role remains to be understood [4]. Moreover, in the structure of CLC-7 an endolysosomal phosphatidylinositol 3-phosphate (PI3P) lipid was found to be bound at the interface between the CBS and the membrane domains [17].

5. Conclusions

While significant progress has been made in elucidating the functional properties of vesicular CLC transporters and their involvement in various neurological diseases, highlighting their importance in nervous system development and homeostasis, their precise physiological role is still largely unknown. Even for the most studied CLC-7, it is still disputed whether it is primarily necessary for proper luminal acidification or the regulation of the luminal chloride concentration. Most recent evidence favors the idea that CLC-7 is responsible for achieving a high luminal chloride concentration, which is important for phagosomal clearance [83]. Less clear are the roles of CLC-3 and CLC-4 in endosomes

and the possible involvement of CIC-3/CIC-4 dimers in human genetic diseases. For all vesicular CLCs, and in particular for CIC-6, the significance of the activation at highly positive voltages remains enigmatic, since similar voltages are not expected to be achieved in endosomes. However, it is clear that CIC-3 and CIC-4 need to be inactive at negative voltages, since even a small amount of activity at these voltages, caused by gate disrupting mutations, leads to severe disease for both transporters [39,41]. In general, it appears that gain of function mutations lead to more severe phenotypes than loss-of function mutations for all vesicular CLCs [39,41,43,49]. In this respect, specific pharmacological inhibitors of vesicular CLCs are highly desirable. Unfortunately, thus far, no useful pharmacological tools are available for any of them.

Author Contributions: M.P. and M.A.C. conceived the idea and prepared the figures. M.A.C., A.T.-M., P.I., P.G., A.L. and M.P. contributed to writing. All authors have read and agreed to the published version of the manuscript.

Funding: This research was partially funded by the European Union—NextGenerationEU (Missione 4 Componente 2, “Dalla ricerca all’impresa”, Innovation Ecosystem RAISE “Robotics and AI for Socio-economic Empowerment”, ECS00000035). However, the views and opinions expressed are those of the authors alone and do not necessarily reflect those of the European Union or the European Commission. Neither the European Union nor the European Commission can be held responsible for them. In addition, this research was partially funded by the Fondazione AIRC per la Ricerca sul Cancro (grant # IG 21558), PRIN-MIUR 2017 Prot. 20174TB8KW, Fondazione Telethon (grant # GMR22T102) granted to M.P. and Fondazione Telethon/Cariplo (grant # GJC22008) to M.P.

Data Availability Statement: Data of Figure 2 are available upon reasonable request.

Acknowledgments: We would like to thank Francesca Quartino and Alessandro Barbin for their excellent technical assistance. This work was partially carried out within the framework of the project “RAISE—Robotics and AI for Socio-economic Empowerment” and has been supported by the European Union—NextGenerationEU.

Conflicts of Interest: The authors declare no conflict of interest.

References

1. Jentsch, T.J.; Pusch, M. CLC chloride channels and transporters: Structure, function, physiology, and disease. *Physiol. Rev.* **2018**, *98*, 1493–1590. [[CrossRef](#)]
2. Jentsch, T.J.; Steinmeyer, K.; Schwarz, G. Primary structure of *Torpedo marmorata* chloride channel isolated by expression cloning in *Xenopus* oocytes. *Nature* **1990**, *348*, 510–514. [[CrossRef](#)] [[PubMed](#)]
3. Accardi, A.; Miller, C. Secondary active transport mediated by a prokaryotic homologue of CIC Cl[−] channels. *Nature* **2004**, *427*, 803–807. [[CrossRef](#)] [[PubMed](#)]
4. Leisle, L.; Ludwig, C.F.; Wagner, F.A.; Jentsch, T.J.; Stauber, T. CIC-7 is a slowly voltage-gated 2Cl[−]/1H⁺-exchanger and requires Ostm1 for transport activity. *EMBO J.* **2011**, *30*, 2140–2152. [[CrossRef](#)] [[PubMed](#)]
5. Middleton, R.E.; Pheasant, D.J.; Miller, C. Homodimeric architecture of a CIC-type chloride ion channel. *Nature* **1996**, *383*, 337–340. [[CrossRef](#)] [[PubMed](#)]
6. Ludewig, U.; Pusch, M.; Jentsch, T.J. Two physically distinct pores in the dimeric CIC-0 chloride channel. *Nature* **1996**, *383*, 340–343. [[CrossRef](#)]
7. Maduke, M.; Pheasant, D.J.; Miller, C. High-level expression, functional reconstitution, and quaternary structure of a prokaryotic CIC-type chloride channel. *J. Gen. Physiol.* **1999**, *114*, 713–722. [[CrossRef](#)] [[PubMed](#)]
8. Mindell, J.A.; Maduke, M.; Miller, C.; Grigorieff, N. Projection structure of a CIC-type chloride channel at 6.5 Å resolution. *Nature* **2001**, *409*, 219–223. [[CrossRef](#)]
9. Dutzler, R.; Campbell, E.B.; Cadene, M.; Chait, B.T.; MacKinnon, R. X-ray structure of a CIC chloride channel at 3.0 Å reveals the molecular basis of anion selectivity. *Nature* **2002**, *415*, 287–294. [[CrossRef](#)]
10. Dutzler, R.; Campbell, E.B.; MacKinnon, R. Gating the selectivity filter in CIC chloride channels. *Science* **2003**, *300*, 108–112. [[CrossRef](#)]
11. Ponting, C.P. CBS domains in CIC chloride channels implicated in myotonia and nephrolithiasis (kidney stones). *J. Mol. Med.* **1997**, *75*, 160–163.
12. Estévez, R.; Jentsch, T.J. CLC chloride channels: Correlating structure with function. *Curr. Opin. Struct. Biol.* **2002**, *12*, 531–539. [[CrossRef](#)]
13. Meyer, S.; Dutzler, R. Crystal structure of the cytoplasmic domain of the chloride channel CIC-0. *Structure* **2006**, *14*, 299–307. [[CrossRef](#)]

14. Meyer, S.; Savaresi, S.; Forster, I.C.; Dutzler, R. Nucleotide recognition by the cytoplasmic domain of the human chloride transporter ClC-5. *Nat. Struct. Mol. Biol.* **2007**, *14*, 60–67. [[CrossRef](#)]
15. Markovic, S.; Dutzler, R. The structure of the cytoplasmic domain of the chloride channel ClC-Ka reveals a conserved interaction interface. *Structure* **2007**, *15*, 715–725. [[CrossRef](#)]
16. Bateman, A. The structure of a domain common to archaeobacteria and the homocystinuria disease protein. *Trends Biochem. Sci.* **1997**, *22*, 12–13. [[CrossRef](#)]
17. Schrecker, M.; Korobenko, J.; Hite, R.K. Cryo-EM structure of the lysosomal chloride-proton exchanger CLC-7 in complex with OSTM1. *eLife* **2020**, *9*, e59555. [[CrossRef](#)] [[PubMed](#)]
18. Park, E.; Campbell, E.B.; MacKinnon, R. Structure of a CLC chloride ion channel by cryo-electron microscopy. *Nature* **2017**, *541*, 500–505. [[CrossRef](#)] [[PubMed](#)]
19. Park, E.; MacKinnon, R. Structure of the CLC-1 chloride channel from *Homo sapiens*. *eLife* **2018**, *7*, e36629. [[CrossRef](#)] [[PubMed](#)]
20. Wang, K.; Preisler, S.S.; Zhang, L.; Cui, Y.; Missel, J.W.; Gronberg, C.; Gotfryd, K.; Lindahl, E.; Andersson, M.; Calloe, K.; et al. Structure of the human ClC-1 chloride channel. *PLoS Biol.* **2019**, *17*, e3000218. [[CrossRef](#)]
21. Pusch, M.; Ludewig, U.; Rehfeldt, A.; Jentsch, T.J. Gating of the voltage-dependent chloride channel ClC-0 by the permeant anion. *Nature* **1995**, *373*, 527–531. [[CrossRef](#)] [[PubMed](#)]
22. Traverso, S.; Elia, L.; Pusch, M. Gating competence of constitutively open CLC-0 mutants revealed by the interaction with a small organic inhibitor. *J. Gen. Physiol.* **2003**, *122*, 295–306. [[CrossRef](#)] [[PubMed](#)]
23. Zifarelli, G.; Murgia, A.R.; Soliani, P.; Pusch, M. Intracellular proton regulation of ClC-0. *J. Gen. Physiol.* **2008**, *132*, 185–198. [[CrossRef](#)]
24. Estévez, R.; Boettger, T.; Stein, V.; Birkenhäger, R.; Otto, E.; Hildebrandt, F.; Jentsch, T.J. Barttin is a Cl[−] channel beta-subunit crucial for renal Cl[−] reabsorption and inner ear K⁺ secretion. *Nature* **2001**, *414*, 558–561. [[CrossRef](#)] [[PubMed](#)]
25. Jeworutzki, E.; López-Hernández, T.; Capdevila-Nortes, X.; Sirisi, S.; Bengtsson, L.; Montolio, M.; Zifarelli, G.; Arnedo, T.; Müller, C.S.; Schulte, U.; et al. GlialCAM, a protein defective in a leukodystrophy, serves as a ClC-2 Cl[−] channel auxiliary subunit. *Neuron* **2012**, *73*, 951–961. [[CrossRef](#)]
26. Jeworutzki, E.; Lagostena, L.; Elorza-Vidal, X.; Lopez-Hernandez, T.; Estevez, R.; Pusch, M. GlialCAM, a CLC-2 Cl[−] channel subunit, activates the slow gate of CLC chloride channels. *Biophys. J.* **2014**, *107*, 1105–1116. [[CrossRef](#)]
27. Lange, P.F.; Wartosch, L.; Jentsch, T.J.; Fuhrmann, J.C. ClC-7 requires Ostm1 as a beta-subunit to support bone resorption and lysosomal function. *Nature* **2006**, *440*, 220–223. [[CrossRef](#)]
28. Stauber, T.; Weinert, S.; Jentsch, T.J. Cell biology and physiology of CLC chloride channels and transporters. *Compr. Physiol.* **2012**, *2*, 1701–1744. [[CrossRef](#)]
29. Bose, S.; He, H.; Stauber, T. Neurodegeneration upon dysfunction of endosomal/lysosomal CLC chloride transporters. *Front. Cell Dev. Biol.* **2021**, *9*, 639231. [[CrossRef](#)]
30. Günther, W.; Lüchow, A.; Cluzeaud, F.; Vandewalle, A.; Jentsch, T.J. ClC-5, the chloride channel mutated in Dent's disease, colocalizes with the proton pump in endocytotically active kidney cells. *Proc. Natl. Acad. Sci. USA* **1998**, *95*, 8075–8080. [[CrossRef](#)]
31. Günther, W.; Piwon, N.; Jentsch, T.J. The ClC-5 chloride channel knock-out mouse—An animal model for Dent's disease. *Pflügers Arch.* **2003**, *445*, 456–462. [[CrossRef](#)]
32. Jentsch, T.J.; Günther, W. Chloride channels: An emerging molecular picture. *Bioessays* **1997**, *19*, 117–126. [[CrossRef](#)] [[PubMed](#)]
33. Piwon, N.; Günther, W.; Schwake, M.; Bösl, M.R.; Jentsch, T.J. ClC-5 Cl[−]-channel disruption impairs endocytosis in a mouse model for Dent's disease. *Nature* **2000**, *408*, 369–373. [[CrossRef](#)]
34. Stobrawa, S.M.; Breiderhoff, T.; Takamori, S.; Engel, D.; Schweizer, M.; Zdebik, A.A.; Bösl, M.R.; Ruether, K.; Jahn, H.; Draguhn, A.; et al. Disruption of ClC-3, a chloride channel expressed on synaptic vesicles, leads to a loss of the hippocampus. *Neuron* **2001**, *29*, 185–196. [[CrossRef](#)] [[PubMed](#)]
35. Weinert, S.; Jabs, S.; Supanchart, C.; Schweizer, M.; Gimber, N.; Richter, M.; Rademann, J.; Stauber, T.; Kornak, U.; Jentsch, T.J. Lysosomal pathology and osteopetrosis upon loss of H⁺-driven lysosomal Cl[−] accumulation. *Science* **2010**, *328*, 1401–1403. [[CrossRef](#)]
36. Ishida, Y.; Nayak, S.; Mindell, J.A.; Grabe, M. A model of lysosomal pH regulation. *J. Gen. Physiol.* **2013**, *141*, 705–720. [[CrossRef](#)] [[PubMed](#)]
37. Lloyd, S.E.; Pearce, S.H.; Fisher, S.E.; Steinmeyer, K.; Schwappach, B.; Scheinman, S.J.; Harding, B.; Bolino, A.; Devoto, M.; Goodyer, P.; et al. A common molecular basis for three inherited kidney stone diseases. *Nature* **1996**, *379*, 445–449. [[CrossRef](#)]
38. Kornak, U.; Kasper, D.; Bösl, M.R.; Kaiser, E.; Schweizer, M.; Schulz, A.; Friedrich, W.; Delling, G.; Jentsch, T.J. Loss of the ClC-7 chloride channel leads to osteopetrosis in mice and man. *Cell* **2001**, *104*, 205–215. [[CrossRef](#)]
39. Duncan, A.R.; Polovitskaya, M.M.; Gaitan-Penas, H.; Bertelli, S.; VanNoy, G.E.; Grant, P.E.; O'Donnell-Luria, A.; Valivullah, Z.; Lovgren, A.K.; England, E.M.; et al. Unique variants in CLCN3, encoding an endosomal anion/proton exchanger, underlie a spectrum of neurodevelopmental disorders. *Am. J. Hum. Genet.* **2021**, *108*, 1450–1465. [[CrossRef](#)]
40. Hu, H.; Haas, S.A.; Chelly, J.; Van Esch, H.; Raynaud, M.; de Brouwer, A.P.; Weinert, S.; Froyen, G.; Frints, S.G.; Laumonnier, F.; et al. X-exome sequencing of 405 unresolved families identifies seven novel intellectual disability genes. *Mol. Psychiatry* **2016**, *21*, 133–148. [[CrossRef](#)]

41. Palmer, E.E.; Pusch, M.; Picollo, A.; Forwood, C.; Nguyen, M.H.; Suckow, V.; Gibbons, J.; Hoff, A.; Sigfrid, L.; Megarbane, A.; et al. Functional and clinical studies reveal pathophysiological complexity of CLCN4-related neurodevelopmental condition. *Mol. Psychiatry* **2023**, *28*, 668–697. [[CrossRef](#)] [[PubMed](#)]
42. Palmer, E.E.; Stuhlmann, T.; Weinert, S.; Haan, E.; Van Esch, H.; Holvoet, M.; Boyle, J.; Leffler, M.; Raynaud, M.; Moraine, C.; et al. De novo and inherited mutations in the X-linked gene CLCN4 are associated with syndromic intellectual disability and behavior and seizure disorders in males and females. *Mol. Psychiatry* **2016**, *23*, 222–230. [[CrossRef](#)] [[PubMed](#)]
43. Polovitskaya, M.M.; Barbini, C.; Martinelli, D.; Harms, F.L.; Cole, F.S.; Calligari, P.; Bocchinfuso, G.; Stella, L.; Ciolfi, A.; Niceta, M.; et al. A Recurrent Gain-of-Function Mutation in CLCN6, Encoding the CIC-6 Cl⁻/H⁺-Exchanger, Causes Early-Onset Neurodegeneration. *Am. J. Hum. Genet.* **2020**, *107*, 1062–1077. [[CrossRef](#)]
44. Poët, M.; Kornak, U.; Schweizer, M.; Zdebek, A.A.; Scheel, O.; Hoelter, S.; Wurst, W.; Schmitt, A.; Fuhrmann, J.C.; Planells-Cases, R.; et al. Lysosomal storage disease upon disruption of the neuronal chloride transport protein CIC-6. *Proc. Natl. Acad. Sci. USA* **2006**, *103*, 13854–13859. [[CrossRef](#)]
45. Zifarelli, G.; Pusch, M.; Fong, P. Altered voltage-dependence of slowly activating chloride-proton antiport by late endosomal CIC-6 explains distinct neurological disorders. *J. Physiol.* **2022**, *600*, 2147–2164. [[CrossRef](#)]
46. He, H.; Cao, X.; Yin, F.; Wu, T.; Stauber, T.; Peng, J. West syndrome caused by a chloride/proton exchange-uncoupling CLCN6 mutation related to autophagic-lysosomal dysfunction. *Mol. Neurobiol.* **2021**, *58*, 2990–2999. [[CrossRef](#)] [[PubMed](#)]
47. Kasper, D.; Planells-Cases, R.; Fuhrmann, J.C.; Scheel, O.; Zeitz, O.; Ruether, K.; Schmitt, A.; Poët, M.; Steinfeld, R.; Schweizer, M.; et al. Loss of the chloride channel CIC-7 leads to lysosomal storage disease and neurodegeneration. *EMBO J.* **2005**, *24*, 1079–1091. [[CrossRef](#)]
48. Pangrazio, A.; Pusch, M.; Caldana, E.; Frattini, A.; Lanino, E.; Tamhankar, P.M.; Phadke, S.; Lopez, A.G.; Orchard, P.; Mihci, E.; et al. Molecular and clinical heterogeneity in CLCN7-dependent osteopetrosis: Report of 20 novel mutations. *Hum. Mutat.* **2010**, *31*, E1071–E1080. [[CrossRef](#)] [[PubMed](#)]
49. Nicoli, E.R.; Weston, M.R.; Hackbarth, M.; Becerril, A.; Larson, A.; Zein, W.M.; Baker, P.R., 2nd; Burke, J.D.; Dorward, H.; Davids, M.; et al. Lysosomal storage and albinism due to effects of a de novo CLCN7 variant on lysosomal acidification. *Am. J. Hum. Genet.* **2019**, *104*, 1127–1138. [[CrossRef](#)]
50. Steinmeyer, K.; Schwappach, B.; Bens, M.; Vandewalle, A.; Jentsch, T.J. Cloning and functional expression of rat CLC-5, a chloride channel related to kidney disease. *J. Biol. Chem.* **1995**, *270*, 31172–31177. [[CrossRef](#)]
51. Friedrich, T.; Breiderhoff, T.; Jentsch, T.J. Mutational analysis demonstrates that CIC-4 and CIC-5 directly mediate plasma membrane currents. *J. Biol. Chem.* **1999**, *274*, 896–902. [[CrossRef](#)]
52. Guzman, R.E.; Grieschat, M.; Fahlke, C.; Alekov, A.K. CIC-3 is an intracellular chloride/proton exchanger with large voltage-dependent nonlinear capacitance. *ACS Chem. Neurosci.* **2013**, *4*, 994–1003. [[CrossRef](#)] [[PubMed](#)]
53. Guzman, R.E.; Miranda-Laferte, E.; Franzen, A.; Fahlke, C. Neuronal CIC-3 splice variants differ in subcellular localizations, but mediate identical transport functions. *J. Biol. Chem.* **2015**, *290*, 25851–25862. [[CrossRef](#)] [[PubMed](#)]
54. Stauber, T.; Jentsch, T.J. Sorting motifs of the endosomal/lysosomal CLC chloride transporters. *J. Biol. Chem.* **2010**, *285*, 34537–34548. [[CrossRef](#)] [[PubMed](#)]
55. Zifarelli, G.; Pusch, M. Conversion of the 2 Cl⁻/1 H⁺ antiporter CIC-5 in a NO₃⁻/H⁺ antiporter by a single point mutation. *Embo J.* **2009**, *28*, 175–182. [[CrossRef](#)]
56. Li, X.; Shimada, K.; Showalter, L.A.; Weinman, S.A. Biophysical properties of CIC-3 differentiate it from swelling-activated chloride channels in Chinese hamster ovary-K1 cells. *J. Biol. Chem.* **2000**, *275*, 35994–35998. [[CrossRef](#)]
57. Zifarelli, G.; Pusch, M. Intracellular regulation of human CIC-5 by adenine nucleotides. *EMBO Rep.* **2009**, *10*, 1111–1116. [[CrossRef](#)]
58. De Stefano, S.; Pusch, M.; Zifarelli, G. Extracellular determinants of anion discrimination of the Cl⁻/H⁺ antiporter CLC-5. *J. Biol. Chem.* **2011**, *286*, 44134–44144. [[CrossRef](#)]
59. Picollo, A.; Pusch, M. Chloride/proton antiporter activity of mammalian CLC proteins CIC-4 and CIC-5. *Nature* **2005**, *436*, 420–423. [[CrossRef](#)]
60. De Stefano, S.; Pusch, M.; Zifarelli, G. A single point mutation reveals gating of the human CIC-5 Cl⁻/H⁺ antiporter. *J. Physiol.* **2013**, *591*, 5879–5893. [[CrossRef](#)]
61. Dickerson, L.W.; Bonthius, D.J.; Schutte, B.C.; Yang, B.; Barna, T.J.; Bailey, M.C.; Nehrke, K.; Williamson, R.A.; Lamb, F.S. Altered GABAergic function accompanies hippocampal degeneration in mice lacking CIC-3 voltage-gated chloride channels. *Brain Res.* **2002**, *958*, 227–250. [[CrossRef](#)]
62. Yoshikawa, M.; Uchida, S.; Ezaki, J.; Rai, T.; Hayama, A.; Kobayashi, K.; Kida, Y.; Noda, M.; Koike, M.; Uchiyama, Y.; et al. CLC-3 deficiency leads to phenotypes similar to human neuronal ceroid lipofuscinosis. *Genes Cells* **2002**, *7*, 597–605. [[CrossRef](#)] [[PubMed](#)]
63. Guzman, R.E.; Bungert-Plumke, S.; Franzen, A.; Fahlke, C. Preferential association with CIC-3 permits sorting of CIC-4 into endosomal compartments. *J. Biol. Chem.* **2017**, *292*, 19055–19065. [[CrossRef](#)] [[PubMed](#)]
64. Weinert, S.; Gimber, N.; Deuschel, D.; Stuhlmann, T.; Puchkov, D.; Farsi, Z.; Ludwig, C.F.; Novarino, G.; Lopez-Cayuqueo, K.I.; Planells-Cases, R.; et al. Uncoupling endosomal CLC chloride/proton exchange causes severe neurodegeneration. *EMBO J.* **2020**, *39*, e103358. [[CrossRef](#)] [[PubMed](#)]

65. Veeramah, K.R.; Johnstone, L.; Karafet, T.M.; Wolf, D.; Sprissler, R.; Salogiannis, J.; Barth-Maron, A.; Greenberg, M.E.; Stuhlmann, T.; Weinert, S.; et al. Exome sequencing reveals new causal mutations in children with epileptic encephalopathies. *Epilepsia* **2013**, *54*, 1270–1281. [[CrossRef](#)]
66. He, H.; Guzman, R.E.; Cao, D.; Sierra-Marquez, J.; Yin, F.; Fahlke, C.; Peng, J.; Stauber, T. The molecular and phenotypic spectrum of CLCN4-related epilepsy. *Epilepsia* **2021**, *62*, 1401–1415. [[CrossRef](#)] [[PubMed](#)]
67. Brandt, S.; Jentsch, T.J. CIC-6 and CIC-7 are two novel broadly expressed members of the CLC chloride channel family. *FEBS Lett.* **1995**, *377*, 15–20. [[CrossRef](#)]
68. Ignoul, S.; Simaels, J.; Hermans, D.; Annaert, W.; Eggermont, J. Human CIC-6 is a late endosomal glycoprotein that associates with detergent-resistant lipid domains. *PLoS ONE* **2007**, *2*, e474. [[CrossRef](#)]
69. Neagoe, I.; Stauber, T.; Fidzinski, P.; Bergsdorf, E.Y.; Jentsch, T.J. The late endosomal CIC-6 mediates proton/chloride counter-transport in heterologous plasma membrane expression. *J. Biol. Chem.* **2010**, *285*, 21689–21697. [[CrossRef](#)]
70. Kobertz, W.R. Want to hear CIC-6 sing? Push your amp to eleven. *J. Physiol.* **2022**, *600*, 2019–2020. [[CrossRef](#)]
71. Pusch, M.; Zifarelli, G. Large transient capacitive currents in wild-type lysosomal Cl^-/H^+ antiporter CIC-7 and residual transport activity in the proton glutamate mutant E312A. *J. Gen. Physiol.* **2021**, *153*, e202012583. [[CrossRef](#)] [[PubMed](#)]
72. Graves, A.R.; Curran, P.K.; Smith, C.L.; Mindell, J.A. The Cl^-/H^+ antiporter CIC-7 is the primary chloride permeation pathway in lysosomes. *Nature* **2008**, *453*, 788–792. [[CrossRef](#)] [[PubMed](#)]
73. Ludwig, C.F.; Ullrich, F.; Leisle, L.; Stauber, T.; Jentsch, T.J. Common gating of both CLC transporter subunits underlies voltage-dependent activation of the $2\text{Cl}^-/\text{H}^+$ exchanger CIC-7/Ostm1. *J. Biol. Chem.* **2013**, *288*, 28611–28619. [[CrossRef](#)] [[PubMed](#)]
74. Smith, A.J.; Lippiat, J.D. Voltage-dependent charge movement associated with activation of the CLC-5 $2\text{Cl}^-/\text{H}^+$ exchanger. *Faseb J.* **2010**, *24*, 3696–3705. [[CrossRef](#)]
75. Zifarelli, G.; De Stefano, S.; Zanardi, I.; Pusch, M. On the mechanism of gating charge movement of CIC-5, a human Cl^-/H^+ antiporter. *Biophys. J.* **2012**, *102*, 2060–2069. [[CrossRef](#)]
76. Chalhoub, N.; Benachenhou, N.; Rajapurohitam, V.; Pata, M.; Ferron, M.; Frattini, A.; Villa, A.; Vacher, J. Grey-lethal mutation induces severe malignant autosomal recessive osteopetrosis in mouse and human. *Nat. Med.* **2003**, *9*, 399–406. [[CrossRef](#)]
77. Pata, M.; Héraud, C.; Vacher, J. OSTM1 bone defect reveals an intercellular hematopoietic crosstalk. *J. Biol. Chem.* **2008**, *283*, 30522–30530. [[CrossRef](#)]
78. Wartosch, L.; Fuhrmann, J.C.; Schweizer, M.; Stauber, T.; Jentsch, T.J. Lysosomal degradation of endocytosed proteins depends on the chloride transport protein CIC-7. *FASEB J.* **2009**, *23*, 4056–4068. [[CrossRef](#)]
79. Sartelet, A.; Stauber, T.; Coppieters, W.; Ludwig, C.F.; Fasquelle, C.; Druet, T.; Zhang, Z.; Ahariz, N.; Cambisano, N.; Jentsch, T.J.; et al. A missense mutation accelerating the gating of the lysosomal Cl^-/H^+ -exchanger CIC-7/Ostm1 causes osteopetrosis with gingival hamartomas in cattle. *Dis. Model Mech.* **2014**, *7*, 119–128. [[CrossRef](#)]
80. Di Zanni, E.; Palagano, E.; Lagostena, L.; Strina, D.; Rehman, A.; Abinun, M.; De Somer, L.; Martire, B.; Brown, J.; Kariminejad, A.; et al. Pathobiologic Mechanisms of Neurodegeneration in Osteopetrosis Derived From Structural and Functional Analysis of 14 CIC-7 Mutants. *J. Bone Miner. Res.* **2021**, *36*, 531–545. [[CrossRef](#)]
81. Leray, X.; Hilton, J.K.; Nwangwu, K.; Becerril, A.; Mikusevic, V.; Fitzgerald, G.; Amin, A.; Weston, M.R.; Mindell, J.A. Tonic inhibition of the chloride/proton antiporter CIC-7 by PI(3,5)P2 is crucial for lysosomal pH maintenance. *eLife* **2022**, *11*, e74136. [[CrossRef](#)] [[PubMed](#)]
82. Zhang, S.; Liu, Y.; Zhang, B.; Zhou, J.; Li, T.; Liu, Z.; Li, Y.; Yang, M. Molecular insights into the human CLC-7/Ostm1 transporter. *Sci. Adv.* **2020**, *6*, eabb4747. [[CrossRef](#)] [[PubMed](#)]
83. Wu, J.Z.; Zeziulia, M.; Kwon, W.; Jentsch, T.J.; Grinstein, S.; Freeman, S.A. CIC-7 drives intraphagosomal chloride accumulation to support hydrolase activity and phagosome resolution. *J. Cell Biol.* **2023**, *222*, e202208155. [[CrossRef](#)] [[PubMed](#)]

Disclaimer/Publisher's Note: The statements, opinions and data contained in all publications are solely those of the individual author(s) and contributor(s) and not of MDPI and/or the editor(s). MDPI and/or the editor(s) disclaim responsibility for any injury to people or property resulting from any ideas, methods, instructions or products referred to in the content.